

# New approaches to nonlinear diffractive field propagation

R. T. Christensen, Fred K. Quin, J. Barker

*Department of Electrical Engineering and Rochester Center for Biomedical Ultrasound, University*

*of Rochester, Rochester, New York 14627*

*(Received 26 September 1989; revised 12 February; accepted 18 February 1991)*

In many domains of acoustic field propagation, such as medical ultrasound imaging, lithotripsy shock treatment, and underwater sonar, a realistic calculation of beam patterns requires treatment of the effects of diffraction from finite sources. Also, the mechanisms of loss and nonlinear effects within the medium are typically nonnegligible. The combination of

and numerical techniques. A novel model that incrementally propagates the fields of baffled planar sources with substeps that account for the physics of diffraction, attenuation, and nonlinearity is presented. The model accounts for the effects of refraction and reflection (but not multiple reflections) in the case of propagation through multiple, parallel layers of fluid medium. An implementation of the model for axis-symmetric sources has been developed. In

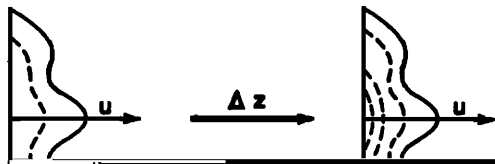
problem, in order to gain advantages in computational efficiency, to develop a formalism that does not require the parabolic approximation, and to allow for multiple layer propagations. Basically, our methodology utilizes an incremental propagation of an axially symmetric field from some

equivalent incremental  $\Delta z$  distance without diffraction, but with accretion and depletion of harmonics according to a temporal frequency domain solution to Burgers' equation (FDSBE).<sup>20-22</sup> That is, for some radial position  $r_i$ , the normal derivative of the axial velocity is modified by the

plane at axial distance  $z$  from the source to a parallel plane at distance  $z + \Delta z$ . The concept is illustrated in Fig. 1. The axial velocity radial profiles  $u(z, r)$  of a fundamental

mechanisms to  $u_n(z + \Delta z, r_i)$  as if the acoustic velocity represented a plane wave traveling in the direction of the phase

NONLINEAR SUBSTEP



$$H_n(\Delta z, R)$$

$$= \begin{cases} \exp[j2\pi\Delta z\sqrt{(nf/c)^2 - R^2}], & |R| < nf/c, \\ \exp[-2\pi\Delta z\sqrt{R^2 - (nf/c)^2}], & |R| > nf/c. \end{cases} \quad (2)$$

An approach based on the sampling of  $H_n(\Delta z, R)$  is computationally simpler since it doesn't require the discrete Hankel transforming of the  $h_n$  functions. If nonaxis symmetric

where  $\beta$  is the nonlinear parameter  $1 + (1/2)B/A$ ,  $f$  is the fundamental frequency, and  $u_n(z + \Delta z, i)$  denotes the  $n$ th term in an  $N$  term complex Fourier series describing the temporal normal velocity waveform at the  $i$ th radial field

the step size requirements drop roughly in proportion to  $N$ , thus making the overall complexity of the FDSBE-based nonlinear (plane-wave) propagation approximately  $N^3$  (Ref. 23). Combining this with the  $N^2$  complexity of the

portion terms the  $u_n(z + \Delta z, i)$  terms have been abbreviated the number of radial samples  $N$  needed since roughly in pro

$$S = \sum_1^N 2I_n \alpha (nf)^{b(n)},$$

(6) The radial sampling rate of the field should be large enough to describe the significant spatial frequency content

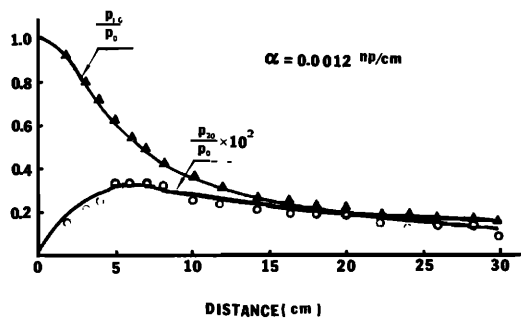


FIG. 4. Comparison with the measured and computed, unfocused Gaussian, axial harmonic pressure amplitudes of Du and Breazeale (1985). (a) Their axial results, note the scaling of the second harmonic. (b) Our computed results (using the same scaling).

corresponding results from our model (using 50 harmonics) are shown in Fig. 6(b). The model's normal velocity output has been converted to pressure using the impedance relation. Baker *et al.*'s log scaled second and third harmonic amplitudes, as measured and predicted, are shown in Figs. 7(a)

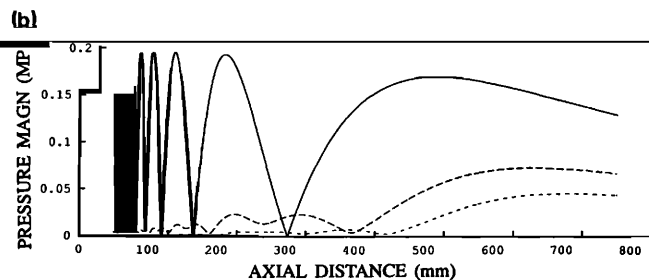
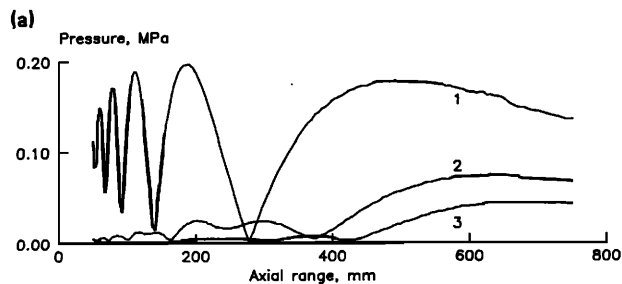
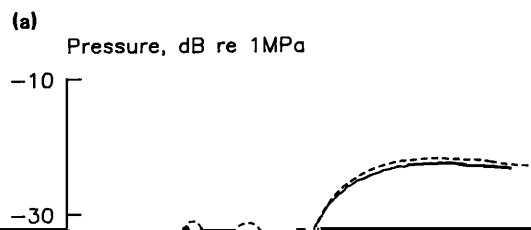


FIG. 6. Comparison with the measured axial harmonic pressure amplitudes of Baker *et al.* for an unfocused 2.25-MHz piston transducer. (a) First three measured harmonic amplitudes. (b) Corresponding computed results from our model.

and 8(a), respectively. The near-field errors in their predicted second and third harmonic amplitudes are consistent with the limitations of the parabolic approximation.<sup>27</sup> Figures 7(b) and 8(b) display the corresponding predictions of



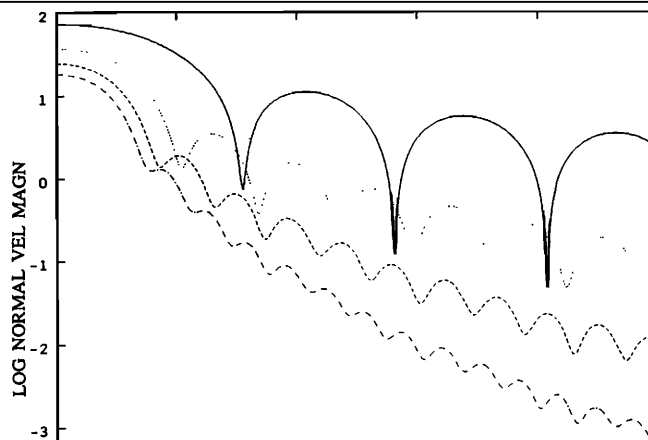
Pressure, dB re 1MPa

-20-

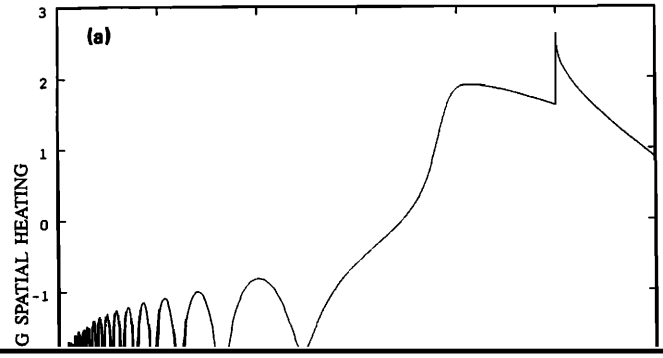
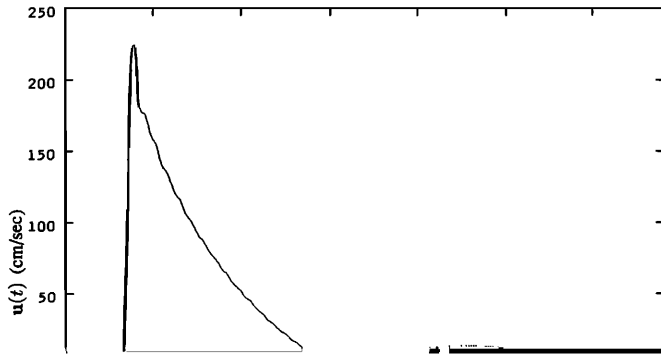
agree with the measurements in the near field and the far field. The far-field agreement is best seen in comparing Fig.

directionalities of the fundamental and higher harmonics were parallel to the  $z$  axis over the radial range of interest and thus no differential directionalities amongst the harmonics existed (which is not accounted for in our model). Figure 9(c) is an expanded depiction of the computed results shown in Fig. 9(b). Note the well formed sidelobes of the second and third harmonics.

In the companion linear paper,<sup>19</sup> the field of a 3-MHz focused piston source operating in a water medium and in a layered fat/liver, biomedical imaging medium was considered [see Fig. 9(a) and (b)]. The water medium had parameters  $c = 1500$  m/s,  $\rho = 1.0$  g/cm<sup>3</sup>,  $\alpha = 0.00025$  Np/cm, and  $b = 2$ . The two-layer medium consisted of 2 cm of fat with parameters  $c = 1460$  m/s,  $\rho = 0.95$  g/cm<sup>3</sup>,  $\alpha = 0.15$







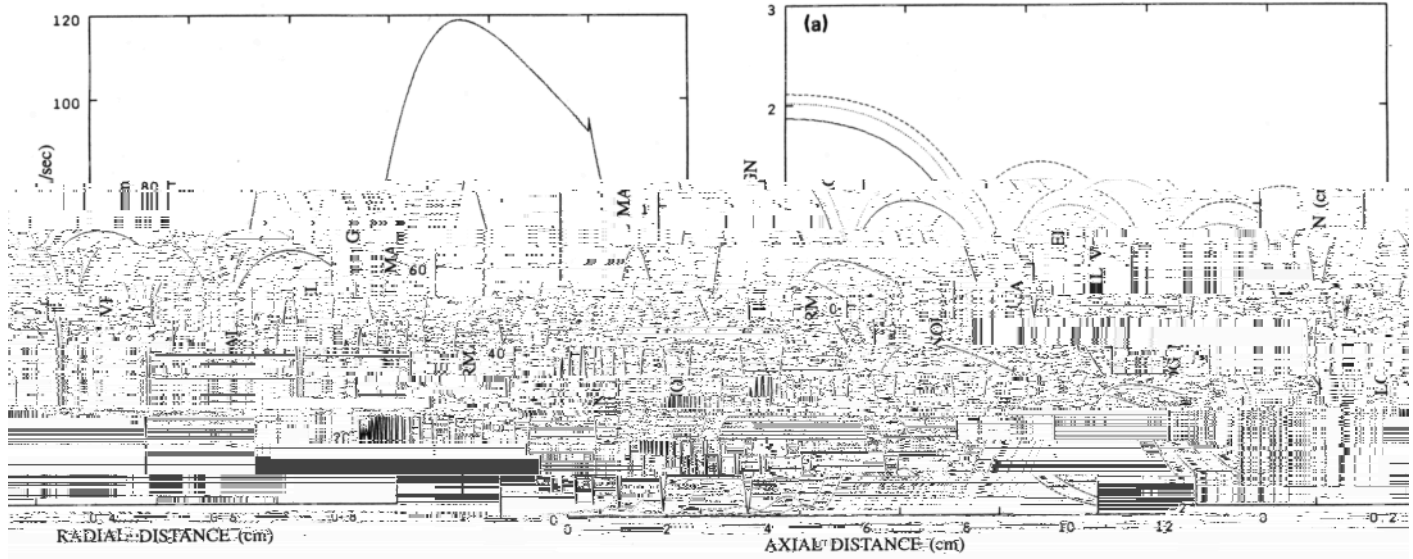
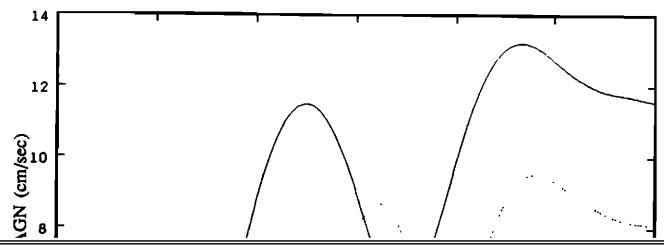
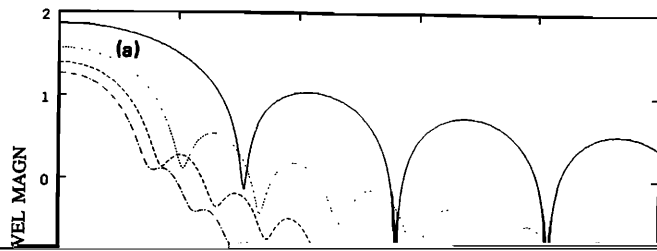


FIG. 17. Fundamental and fourth harmonic focal plane radial amplitudes for the 3-MHz focused piston transducer operating at 3, 10, and 30 W/cm<sup>2</sup>. (a) Overlay of the fundamental harmonic profiles. Note the shift and loss in depth of the nodes associated with increasing source amplitudes. (b) Overlay of the fourth harmonic profiles. Note the broadening of the main lobes and the "shoulders" visible at 10 and 30 W/cm<sup>2</sup>.

piston transducer of Fig. 13. First four harmonics shown. Note the rapid losses in the fat layer (after a small increase due to the difference in sound speed and density between the two media).

the field enters the highly absorbing medium, it is rapidly attenuated producing a region of high acoustic heating. An example of this phenomenon is displayed in Figs. 13–15. Here, the previously described 3-MHz focused transducer is operated at a source intensity of 6 W/cm<sup>2</sup> with an initial medium of water and a subsequent absorbing layer of fat



plitude profiles are overlaid. Initially, the nodal depth increases near the axis as the source amplitude goes from 3–10 W/cm<sup>2</sup>, then it decreases as the source amplitude goes up to 30 W/cm<sup>2</sup>. Near the axis, the increased source amplitude produces increasing nodal shifts. Far off-axis though, the nodes remain aligned at all three source amplitudes. At intermediate radial distances there are bulges or shoulders in the profiles of the 10 and 30 W/cm<sup>2</sup> fourth harmonic amplitudes. These are located at about  $r = 0.5$  cm and  $r = 0.7$  cm, respectively. These shoulder regions represent the intersection of the near axis, broadened portion of the profile with the far off-axis unshifted portion of the profile

<sup>4</sup>Carl W. Smith and Robert T. Beyer, "Ultrasonic radiation field of a focusing spherical source at finite amplitudes," *J. Acoust. Soc. Am.* **46**, 808–813 (1969).

<sup>5</sup>A. M. Sutin, "Influence of nonlinear effects on the properties of acoustic focusing systems," *Sov. Phys. Acoust.* **24**(4), 334–339 (1978).

<sup>6</sup>N. S. Bakhvalov, Y. A. M. Zhileikin, E. A. Zabolotskaya, and R. V. Khokhlov, "Focused high-amplitude sound beams," *Sov. Phys. Acoust.* **24**(1), 10–15 (1978).

<sup>7</sup>J. C. Lockwood, T. G. Muir, and D. T. Blackstock, "Directive harmonic generation in the radiation field of a circular piston," *J. Acoust. Soc. Am.* **53**, 1148–1153 (1973).

<sup>8</sup>Sigurd I. Aanonsen, T. Barkve, Jaqueline N. Tjøtta, and Sigve Tjøtta, "Distortion and harmonic generation in the nearfield of a finite amplitude sound beam," *J. Acoust. Soc. Am.* **75**, 749–768 (1984).

<sup>9</sup>Mark F. Hamilton, Jaqueline N. Tjøtta, and Sigve Tjøtta, "Nonlinear

Figure 18(a)–(c) depict the first four harmonic, focal plane amplitude profiles of the 3, 10, and 30 W/cm<sup>2</sup> field propagations, respectively. The progressive broadening of

effects in the farfield of a directive sound source," *J. Acoust. Soc. Am.* **78**, 202–216 (1985).

<sup>10</sup>Bernard G. Lucas and Thomas G. Muir, "Field of a finite amplitude focusing beam," *J. Acoust. Soc. Am.* **74**, 1522–1528 (1983).